

Design and Implementation of a 3-Axis 5-Degrees of Freedom Motion Control IoT Workbench for Multi-Parametric Geo-Mechanics Simulators

Hasan Tariq¹

Department of Electrical Engineering
College of Engineering,
Qatar University
Doha, Qatar
hasan.tariq@qu.edu.qa

Abderrazak Abdaoui¹

Department of Electrical Engineering
College of Engineering,
Qatar University
Doha, Qatar
abderrazak.abdaoui@qu.edu.qa

Farid Touati¹

Department of Electrical Engineering
College of Engineering,
Qatar University
Doha, Qatar
touatif@qu.edu.qa

Mohammed Abdulla E Al-Hitmi¹

Department of Electrical Engineering
College of Engineering,
Qatar University
Doha, Qatar
m.a.alhitmi@qu.edu.qa

Damiano Crescini²

Brescia University
Brescia, Italy
damiano.crescini@unibs.it

Adel Ben Manouer³

Canadian University Dubai
Dubai, UAE
adel@tud.ac.ae

Abstract— Natural calamities involving geo-seismic ground motions are a big challenge for disaster management agencies. The accurate event management drill for structure health management requires very precise ground motion control systems to ensure realistic real-time simulation. In this work, a programmable multi-parametric geo-mechanics motion control system is proposed to improve the accuracy, repeatability and remote generation of ground motions. The mechanics of 4 unique seismic waves, one conceptual and one characteristic earthquake was programmed and tested exhibited in the results section. Precise and safe geo-mechanics from 0.1Hz to 120Hz, velocities 3km/h to 25km/h, and terrestrial inclination magnitudes from 10.000° to 10.000° testified the accuracy of the design. This work bridges geophysics, simulation, automation, and state agencies for calibrating their seismic sensors, training their event detection algorithm and improve their disaster management drills.

Keywords— automation, geo-mechanics, realization, motion control system, drivers, motors, earthquake, programmable, simulation, calibration, machine learning.

I. INTRODUCTION

The natural disasters occur on the globe every year with earthquake and floods being most devastating and horrible on the loss and damage benchmarks. The number of people reported affected by natural disasters 564.4million in 2006 [1], natural disaster economic damages (US\$ 154 billion), and 12% above the 2006-2015 annual average [2] registered in CRED database. The top chart [3] was in Indonesia on September 28, 2018 with 2,256 death tolls.

An accurate and precise early seismic warning and disaster management (ESWDM) needs a trustable ground motion simulator for training and realization purposes. In recent works, the generic [4] earthquake testbench, the GG SCHIERLE [5] shake table with spring-loaded mechanism, myQuake [6], the world's largest [7] ground motion simulator (GMS), second largest earthquake facility [8], and the State Key Laboratory for Disaster Reduction in Civil Engineering, Tongji University with reference shake [9] table needed improvement in constraint coordination in electro-mechanical optimization on motion control grounds. The [10] shake table with a motor shaft based motion control mechanism in UC, Berkley needed multi-sensor filtering and

verification with more degrees of freedom (DoF). The shake table [11], the Petascale [12], and the collaborative design [13] optimization shake tables work had a common gap of comparative studies and standardization procedures used in [14-17] for real-world earthquakes [18-22] with highest death tolls. The simulators presented in [4-17] had a gap of motion control system accuracy and measurement noise filtration using a multi-sensing mechanism. The four shake tables studied by [23], i.e. National Technical University of Athens shaking table, Bristol University shaking table, the ISMES MASTER shaking table, and the 3D LNEC shaking table with a common gaps of motion control optimization and noise compensation using dynamic filtering [24] work.

The target gaps that need to be addressed are mechanical design in terms more of degrees of freedom (DOF), motion control intelligence, power efficiency, web and IoT control with accuracy in P and S wave generation. This work focuses on a programmable multi-parametric 3-axis 5-DOF motion control IoT workbench (MCW) benchmarked using a 24-bit delta-sigma high-resolution node, and is organized as:

- 3-Axis 5-DoF Motion Control Workbench (MCW) Design and Development
- MCW Optimization Algorithm (MOA)
- High Precision 3D Motion and Position Benchmarking Differential IoT Smart Nodes (MPDNs) Setup
- Multi-variable frequency (position, motion) noise discrimination filter (MNCF)

II. MCW SYSTEM DESIGN AND DEVELOPMENT

The MCW is a constraint mechatronic system specially designed and implemented for geo-seismic ground motions in three different axis orientations. The overall functional layout of MCW is given in figure 1 with the flow of data.

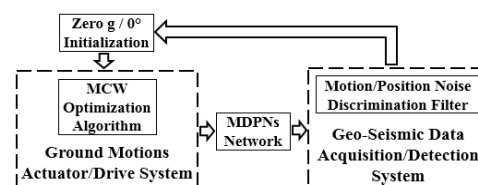


Fig 1. Functional Block Diagram of MCW

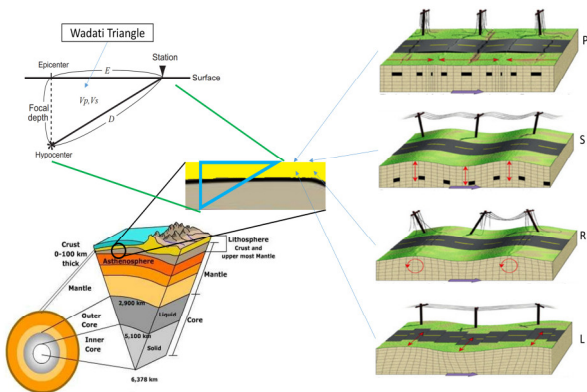


Fig 2. Conceptual Overview of Geo-Mechanics

The conceptual layout of geo-mechanics for geo-seismic waves is given in figure 2. In figure 2, the geo-mechanics of four waves is ambient as red. The geo-seismic motion of four waves was made possible only with red arrows. Five unique motions can be observed from this diagram with different inertial frames and flexibility constraints. The entire geo-mechanics study revolved around refractive seismology based on the Wadati triangle using triangulation axioms. The cumulative topology of assemblies used in recent work was geological domain centered and also published on our previous works [13]. A 3-axis motion platform is exhibited in figure 3 with the design melioration performed in 4-DoF to achieve accurate geo-seismic motions for 5-DoF.

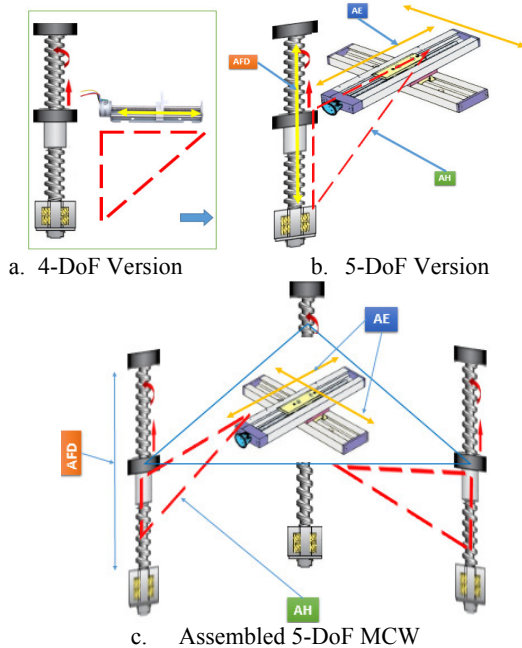


Fig 3. Comparison of Overview of Geo-Mechanics

The 5-DoF MCW consists of two electro-mechanical subsystems that act like an actuator-sensor synergic framework. The two components of MCW are:

- Geo-seismic mechanics actuators-drive system (GMAS)
- Heterogeneous Geo-Seismic Sensing System (HGSS)

A. Geo-seismic mechanics actuators-drive system (GMAS)

Two unique motor sets with two unique motion requirements were used for vertically and horizontally

coordinated mechanics. The bipolar stepper motors type1 and type2 specified in work were optimized in terms of motion control for accurate geo-mechanics are exhibited in figures 2 and 3 using A4988 at 3 different current adjustments for variable torque requirements. The RPM and acceleration programming was also a novel task performed in this work for geo-mechanics. The motion control system consists of an ESP32 an Xtensa II 32-Bit SoC coupled with A4988 stepper drivers with micro-stepping capabilities and 12V/2A power supply drive for bi-polar stepper motors. The overall system layout is given in figure 3.

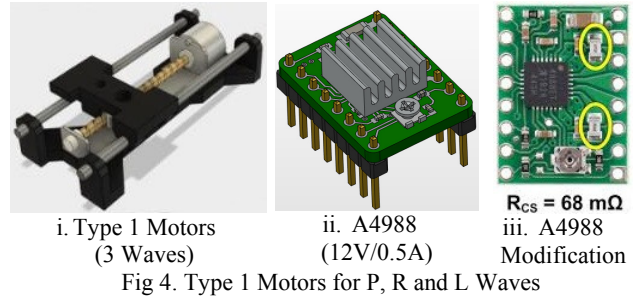


Fig 4. Type 1 Motors for P, R and L Waves

Two Type 1 motors (figure 4) were used at the surface plate in blue color in figure 2 for AE sub-assembly for motion represented with yellow lines.

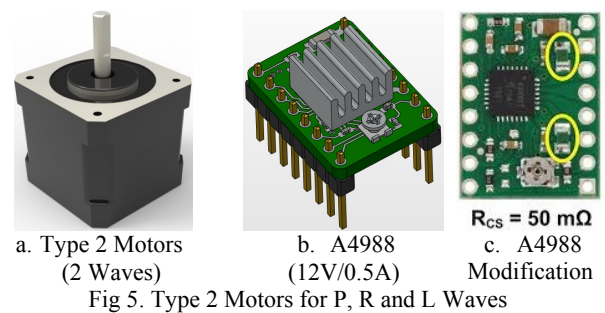


Fig 5. Type 2 Motors for P, R and L Waves

Three Type 2 motors (figure 5) were used at vertical threaded rod sub-assembly AFD with yellow vertical line and in figure 2 for motion represented with red lines.

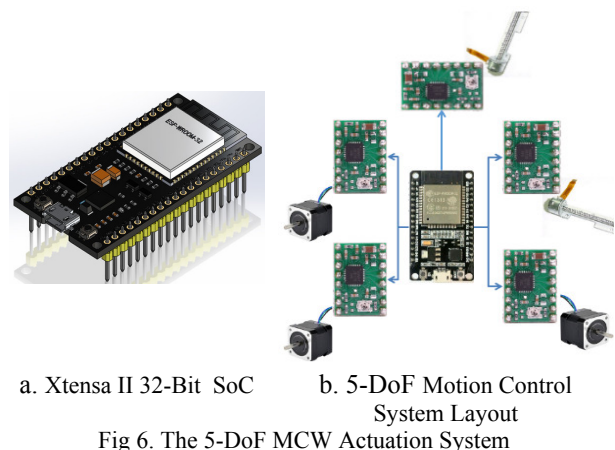
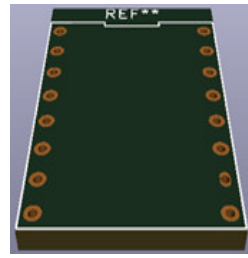


Fig 6. The 5-DoF MCW Actuation System

In figure 6, a five actuators control system with a current control setting optimized for the desired range of geo-seismic magnitudes M1 to M10, i.e. 0.5A (68mΩ) for two motors in AE assembly and three motors with 1A (50mΩ) in AFD for A4988 bipolar stepper drivers.

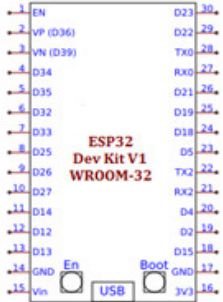
Inputs	1	ENABLE	VMOT	9	Power Input
Inputs	2	MS1	GND	10	Input
Inputs	3	MS2	2B	11	Output
Inputs	4	MS3	2A	12	Output
Inputs	5	RESET	1A	13	Output
Inputs	6	SLEEP	1B	14	Output
Inputs	7	STEP	VDD	15	Power Input
Inputs	8	DIR	GND	16	Input

A4988

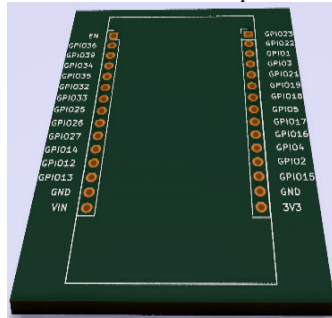


i. A4988 Schematic

ii. A4988 PCB Footprint



iii. Xtenxa II Schematic



iv. Xtenxa II PCB Footprint

Fig 7. The 5-DoF MCW EDA Component Models

For complete system fabrication, the schematic symbols were designed in Proteus 8.6 ISIS and KiCAD 4 and PCB footprints were designed in FreeCAD presented in figure 7. These footprints were imported as .step files in KiCAD to finalize the MCW system design.

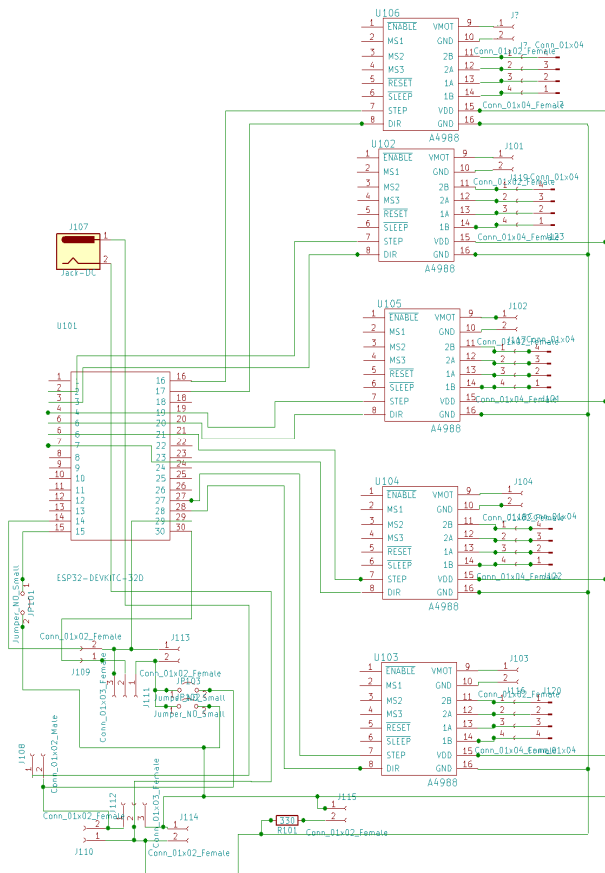
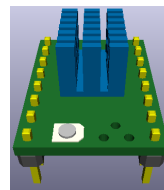
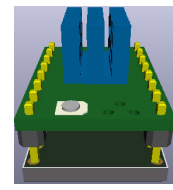


Fig 8. Detailed Schematic Layout of MCW

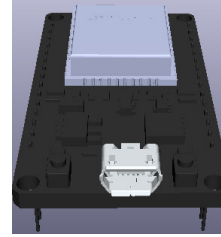
In figure 8, a complete all auxiliary headers for troubleshooting and calibration requirements.



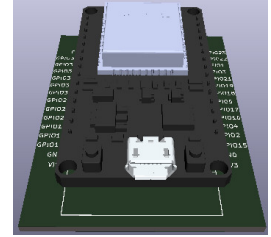
i. A4988 FreeCAD Model



ii. A4988 3D Alignment



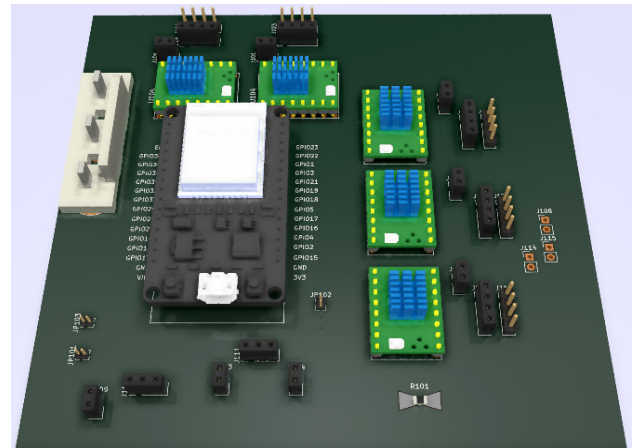
iii. Xtenxa II FreeCAD Model



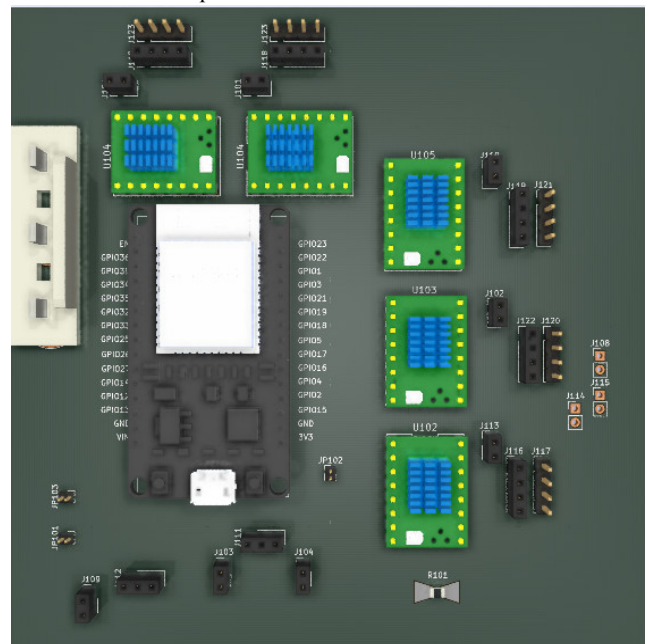
iv. Xtenxa II 3D Alignment

Fig 9. The 5-DoF MCW EDA Component Models

The last challenge in EDA of MCW GMAS electronics was the alignment of 3D models of components, i.e. five A4988 and one Xtenxa II in PCB assembly presented in figure 9. It was performed in Proteus 8.6 ARES as well as KiCAD 4.



i. 3D Perspective View of MCW-GMAS Motherboard



i. Top View of MCW-GMAS Motherboard
Fig 10. Two Views of MCW-GMAS Motherboard

A complete MCW-GMAS motherboard is shown in figure 10. The type I motors were driven by U104 A4988 modules and type II by U102, U103 and U105 A4988 modules. The white power connector was fed with +12V at the top pin for motors drivers, +5V for Xtensa II at middle pin, and ground at lower pin.

B. MCW Optimization Algorithm (MOA)

The MOA is the core firmware components for safe and optimized operation of motion control focused on geo-mechanics. MOA is loaded as the first thread in the firmware at boot time. MOA flowchart is given in figure 11. The MOA follows a sequential methodology of operations given as:

1. When System is powered on, an access point is created, then AP is created after the acquisition of IP address. After a stable webserver creation, the GMSP loads associated pages from SPIFFS for its user interactive web interface (explained in later sections).
2. After AP and web server operations, it takes inputs from MPDN and brings itself into zero "g" condition i.e. removes all the initial value offsets using the SON mechanism. Motors operate till it's zero acceleration and displacement is at 0° tilt.
3. The MOA is stored as a binary code in firmware of SoC and is ready to receive user commands that simulate geo-mechanics.

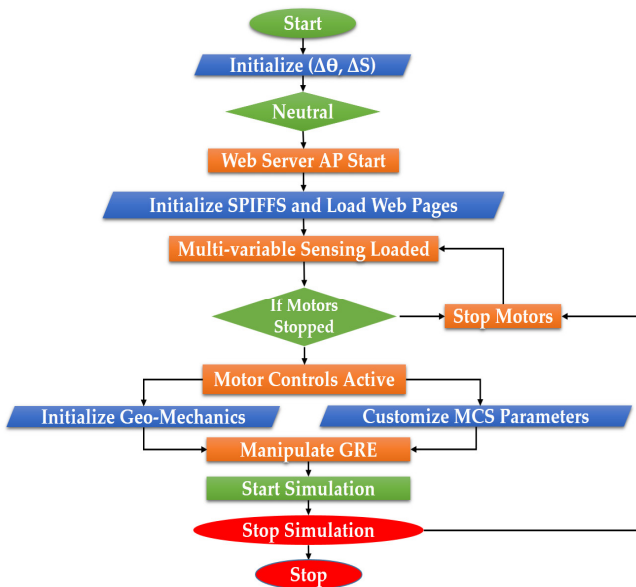


Fig 11. Flowchart of the MOA

Figure 11 summarized a comprehensive flowchart of the MOA explained below for an MCW as well as all the IoT based geo-mechanics simulators with native Web interface:

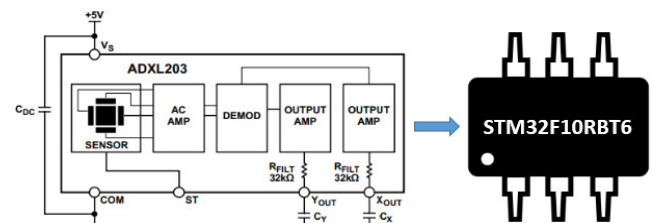
1. The first step after booting is creating MCW access point. Both options are available as station as well as an access point. This work is based on access point mode.
2. The second step is the creation of IoT Web Server and loads web pages stored on MCW firmware.

3. The third step consists of posting the sensor variables to webpages.
4. Step four is normalizing the AE to 0° tilt-angle and move the MPDN to origin so that there are no offsets with the help of instrumentation support.
5. In step five, the MPDN Dashboard page is loaded with current tilt-angles and acceleration magnitudes, all motion variables should be 0.
6. The sixth step is, the MCW gives an indication of "Ready" and is ready to take user inputs if all magnitudes of motion sensors variables are 0 with a tolerance of $\pm 0.00X$ as practically it is impossible to have zero vibration.
7. In step seven, GMAS framework is activated to run and test the last stored motion control commands for MCW. Users can skip step 7 if to enter new commands and control parameters.
8. Step eight is mandatory to fill all the geo-seismic and geo-mechanics parameters for precise specifications of geo-seismic ground motions to manipulate desired geo-mechanics.
9. In step nine the MCW is ready to perform the desired geo-seismic ground motions.

The three great earthquakes datasets can also be loaded in step eight but optional.

C. High Precision 3D Motion and Position Benchmarking Differential IoT Smart Node (MPDN) Setup:

The block diagram of the ADXL203 MEMS chip used as a core component of MDPN is given in figure 12 focusing on the measurement requirements in table 3 of work.



i. ADXL203 Architecture Diagram ii. ADXL MEMS Chip
Fig 12. The ADXL203 Architecture and Fabricated Chip Layout

A bi-axial accelerometer ADXL203 was been used for heterogeneous sensing i.e. acceleration as motion variable in open band with a high-pass filter and low-band for tilt-angles as position variable



i. MDPN PCB



ii. MDPN Fabrication

Fig 13. The MDPN Version 0

In figure 13, the STM32F10RBT6 (32-Bit microcontroller with CAN-Open Transceiver and 24-Bit

delta-sigma ADC with a sampling rate of less than 1 micro-seconds) was interfaced with ADXL203 using two ADC channels to constitute one MDPN secured in IP68 enclosure. A differential measurement setup was used to extract the real ground motion observations free of stepper motor noise consisting of three nodes at three unique planes connected in network presented as red wires in figure 14.

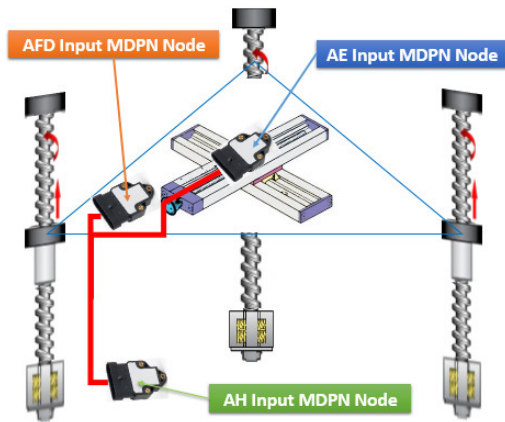


Fig. 14. Motion Control System Layout

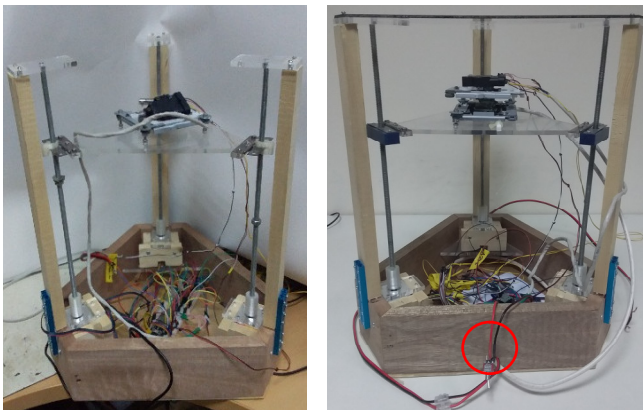
Three nodes were used in the MDPN differential setup (MDS) in figure 13 to optimize the geo-mechanics sensing using a frequency objective function $H(f)$. Let the high-frequency noise in ADF MDPN node that occurs due to internal vibrations of type 2 motors effect on AE surface as $N(f_{ADF})$ and $N(f_{AH})$ at AH assembly in AH MPDN node for positional accuracy. The low-frequency noise $N(f_{AE})$ in AE MDPN node due to high-speed axis movement in AE assembly for motion accuracy. The $H(f)$ as an objective function of multi-variable frequency (position, motion) noise discrimination filter (MNCF) will be the difference of all three nodes unwanted frequencies, given as:

$$H(f) = N(f_{AE}) - N(f_{ADF}) - N(f_{AH}) \quad (1)$$

In equation 1, the $H(f)$ is the automated filtered signal that is almost near to actual ground motion measurements that are free of stepper motor noise.

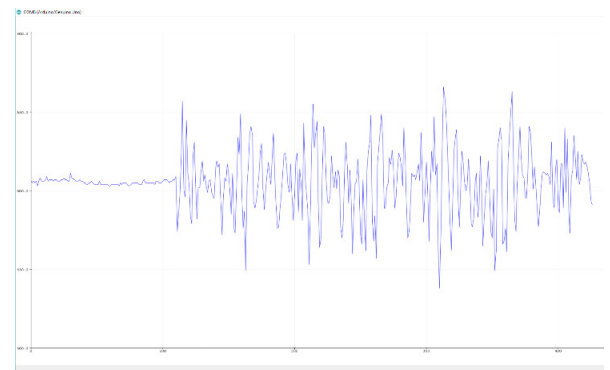
III. RESULTS AND DISCUSSION

The 5-DoF MCW was assembled for performing the experiments as shown in figure 15 as a comparison with previous [13] work.

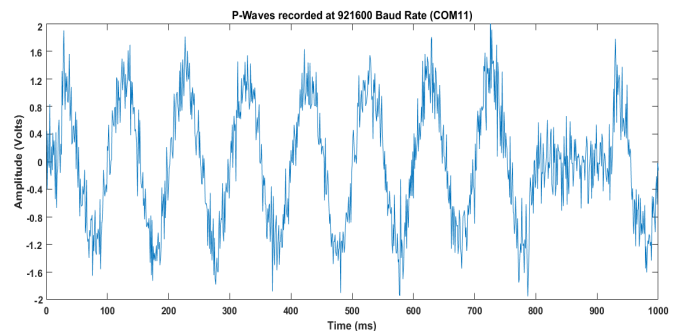


i. GMSP ii. GMSP with MCW
Fig 15. GMSP Assembled Photographs

The results were observed from two sources, i.e. the GMSP and MCW were captured and compared in MATLAB serial input. The MCW results very precise and clear and exhibited in figure 15.

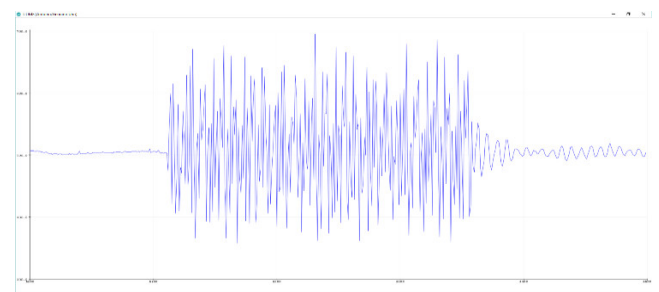


i. P-Waves for 8Hz on the x-axis [16] from GMSP

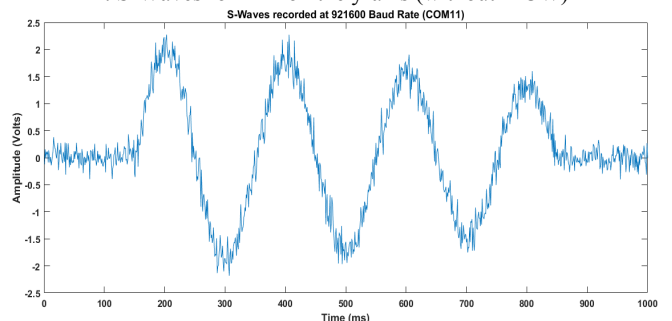


ii. P-Waves for 8Hz on the x-axis from MCW with MOA and MDS
Fig 16. Innovation and Improvement by MCW

Figure 16 portrayed a clear difference in accuracy and meaningful output of MCW on the almost same apparatus with addition DoF and axis.



i. S-Waves for 4Hz on the y-axis (without MCW)



ii. S-Waves for 4Hz on the y-axis from MCW with MOA and MDS

Fig 17. Innovation and Improvement by MCW

The results on MATLAB are very self-explanatory in figure 17(i) and 17(ii) in portraying a clear difference in

innovation. The frequencies achieved by the system are extremely high and show the capability of the system to generate 10 times faster frequencies that were not observed in the literature before.

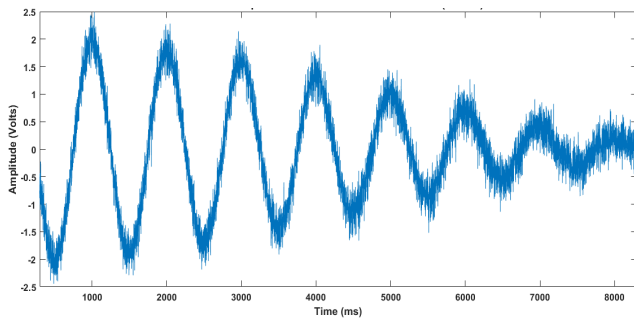


Fig 18. R-Waves for 1Hz on the y-axis from MCW with MOA and MDS

The results on MATLAB were very self-explanatory and picturize an ambient difference in accuracy and fertility of simulations. The frequencies achieved by the system are extremely high and show the capability of the system to generate 10 times faster frequencies that were not observed in the literature before.

Furthermore, a generic or standard earthquake pattern with a classified sequence of seismic waves was programmed on 3-Axis 5-DoF MCW and results are exhibited in figure 19. MCW produced very ideal results in terms of a real earthquake as well as the standard earthquake sequence.

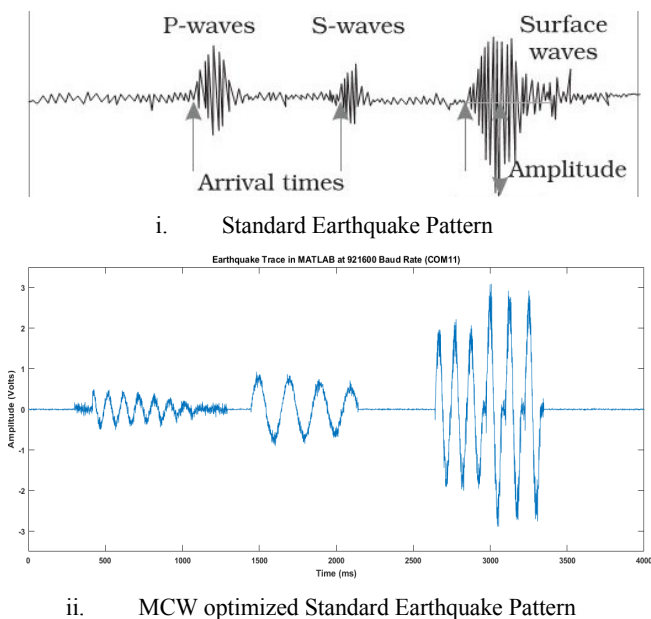


Fig 18. Generic Earthquake Simulation optimized using MCW

The MCW optimized the GMSP generated earthquake from the data collected from the IRIS database and converted into motor controls and programmed into the system as shown in fig 18.

IV. CONCLUSION

An optimized version of multi-parametric 4 degree-of-freedom seismic wave ground motions simulation platform was developed in this work as 3-axis and 5 degrees of freedom with on motors and their respective drives. Three bi-

axial motion and position sensing nodes were used at three different planes in the system to discriminate against the frequency noises. The results highlight the innovation and contribution by optimization of drives on geo-mechanics requirements. The cascaded contribution of mechanical assembly and mechanical workbench optimization algorithm harnessed a focused apparatus for ground motions. The fabricated apparatus was benchmarked by motion and position sensing assisted by noise discrimination realistically contributed to P, S, and Rayleigh waves simulations and standard earthquake sequences. This constituted a strong tool to train algorithms for machine learning and AI as well as deep learning models.

ACKNOWLEDGMENT

This publication was made possible by NPRP grant # 8-1781-2-725 and NPRP grant # 10-0102-170094 from the Qatar National Research Fund (a member of Qatar Foundation). The statements made herein are solely the responsibility of the authors.

REFERENCES

- [1] D. Guha-Sapir, P. Hoyois, P. Wallemacq and R. Below, "Annual Disaster Statistical Review 2016 The numbers and trends," Centre for Research on the Epidemiology of Disasters (CREED), 2016.
- [2] S. Kimball, Earthquake Statistics. United States Geological Survey. Retrieved May 10, 2017.
- [3] Geophysical Journal International, Volume 179, Issue 3, Pages 1669–1678, <https://doi.org/10.1111/j.1365-246X.2009.04363.x>, 2009.
- [4] T. E. Tullis, Keith Richards-Dinger et al, "Generic Earthquake Simulator," Seismological Research Letters, Volume 83, Number 6. 2009.
- [5] A. Velikoseltsev, A. Yankovsky, V. Khvostov, "Implementation of the high accuracy variable rotation testbench: seismology options," in *4th IWGoRS workshop Tutzing*, 2016.
- [6] K. Othani, T. Hayama, N. Ogawa, M. Sato, PROJECT ON 3-D FULL-SCALE EARTHQUAKE TESTING FACILITY, THE FOURTH REPORT, 2006.
- [7] A. Aytun, "A NEW 3-D EARTHQUAKE SIMULATOR FOR TRAINING AND RESEARCH PURPOSES," in *13th World Conference on Earthquake Engineering*, Vancouver, B.C., Canada, Paper No. 3429, 2010.
- [8] K. Yao, W. Huang, C. Lin, P. Wu, J. Chiang, "Virtual Instrumentation Design on Earthquake Simulation System," *International Conference on Artificial Intelligence and Industrial Engineering*, 2015.
- [9] A.N Swaminathan, P.Sankari, "Experimental Analysis of Earthquake Shake Table," *American Journal of Engineering Research*, e-ISSN: 2320-0847 p-ISSN : 2320-0936, Volume-6, Issue-1, pp-148-151, 2017.
- [10] W. Shi, "SHAKING TABLE EXPERIMENTAL STUDY OF REINFORCED CONCRETE HIGH-RISE BUILDING," in *Twelfth World Conference in Earthquake Engineering*, 2012.
- [11] J. E. Barnes, "Seismic Modeling with an Earthquake Shake Table," *DigitalCommons*, 2012.
- [12] S. Pei, "FULL-SCALE SHAKE TABLE TESTING OF A TWOSTORY MASS TIMBER BUILDING WITH RESILIENT ROCKING WALL LATERAL SYSTEM", November 2017.
- [13] H. Tariq, F. Touati, M. Al-Hitmi, A. B. Mnaouer, and D. Crescini, "Design and Implementation of Programmable Multi-Parametric 4-Degrees of Freedom Seismic Waves Ground Motion Simulation IoT Platform," *International Wireless Communications and Mobile Computing Conference*, 2019.
- [14] F. Touati, H. Tariq, D. Crescini, A. B. Manouer, "Design and Simulation of a Green Bi-Variable Mono-Parametric SHM Node and Early Seismic Warning Algorithm for Wave Identification and Scattering," in *14th International Wireless Communications & Mobile Computing Conference*, 2018.

- [15] F. Touati, H. Tariq, A. B. Mnaouer and D. Crescini, "IoT and IoE prototype for scalable infrastructures, architectures and platforms," *International Symposium on Ubiquitous Networking*, pp 202-216, 2018.
- [16] H. Tariq, A. Tahir, F. Touati, M. Al-Hitmi, A. B. Mnaouer, and D. Crescini, "Geographical Area Network—Structural Health Monitoring Utility Computing Model," *International Journal of Geo-Information*, 2019.
- [17] H. Tariq, A. Tahir, F. Touati, M. Al-Hitmi, A. B. Mnaouer, and D. Crescini, "Structural Health Monitoring and Installation Scheme deployment using Utility Computing Model," *European Conference on Electrical Engineering and Computer Science*, 2018.
- [18] H. Tariq, F. Touati, M. Al-Hitmi, A. B. Mnaouer, A. Tahir and D. Crescini, "IoT and IoE prototype for scalable infrastructures, architectures and platforms," *International Robotics & Automation Journal*. 4. 10.15406/iratj.2018.04.00144, 2019.
- [19] H. Tariq, F. Touati, M. Al-Hitmi, A. B. Mnaouer, and D. Crescini, et al, "Design and Implementation of Information Centered Protocol for Long Haul SHM Monitoring," in *International Wireless Communications and Mobile Computing Conference*, 2019.
- [20] A. Galli, F. Touati, M. Al-Hitmi, A. B. Mnaouer, and D. Crescini, "Environmentally Powered Multiparametric Wireless Sensor Node for Air Quality Diagnostic," *Sensors and Materials* 27(2):177-189, January 2015.
- [21] N. Dasyam, "Structural Health Monitoring Market by Component (Hardware, Software, and Services), Connectivity (Wired and Wireless), and End User (Civil, Aerospace, Defense, Energy, and Others)," *Global Opportunity Analysis and Industry Forecast, 2017-2023*.
- [22] U. Asghar et al, "Development of Highly Efficient Multi-Invariable Wireless Sensor System Design for Energy Harvesting," *arXiv:1802.05755*, 2018.
- [23] Engineering, Equipment and Machinery. [online] Allied Market Research, p.201. <https://www.alliedmarketresearch.com/structural-health-monitoring-market>, [Accessed 13 Oct. 2018].
- [24] H. Tariq, F. Touati, M. Al-Hitmi, A. B. Mnaouer, and D. Crescini, A Real-time Early Warning Seismic Event Detection Algorithm using Smart Geo-Spatial Bi-axial Inclinator Nodes for Industry 4.0 Applications, *Applied Sciences*, 2019.